HADRON PRODUCTION AND RADIAL FLOW IN AU+AU COLLISIONS AT RHIC-PHENIX

AKIO KIYOMICHI FOR THE PHENIX COLLABORATION

RIKEN

2-1 Hirosawa, Wako, SAITAMA, 351-0198, Japan

E-mail: kiyo@bnl.gov

The centrality dependence of transverse momentum distributions and yields for $\pi^{\pm}$, $K^{\pm}$, p and $\overline{p}$ in Au+Au collisions at $\sqrt{s_{NN}} = 200$ GeV are measured by the PHENIX experiment at RHIC. The single particle spectra are well fitted with a hydrodynamic-inspired parameterization, termed the "blast-wave" model, to extract freeze-out temperature and radial flow velocity of the particle source. Another motivation is that the suppression of high-p_T hadron as a probe of QGP formation. In central collisions at intermediate transverse momenta $\sim 1.5 - 4.5$ GeV/c, proton and anti-proton yields constitute a significant fraction of the charged hadron production and show a scaling behavior different from that of pions.

1. Introduction

Heavy-ion collisions at high energies offer a unique opportunity to probe highly excited dense nuclear matter in the laboratory. That form of matter is called the quark-gluon plasma (QGP), which is quantum chromodynamics (QCD) analogue of the plasma phase of ordinary atomic matter. Since hadrons contain basic information about collision dynamics, the production of hadrons is one of the important probes of QGP. We present the results of identified hadron spectra and yields in Au+Au collisions [1] at the energy of $\sqrt{s_{NN}} = 200$ GeV by the PHENIX experiment using the Relativistic Heavy Ion Collider (RHIC) at Brookhaven National Laboratory (BNL).

2. Experiments

The PHENIX [2] is one of the major experiments at RHIC to detect a variety of signals from quark-gluon plasma. It is designed to perform a broad study of $A + A$, $p + A$, and $p + p$ collisions to investigate nuclear matter under extreme condition. The detector consists of a large number of subsystems. It comprises two central arms, two forward muon arms, and three global de-
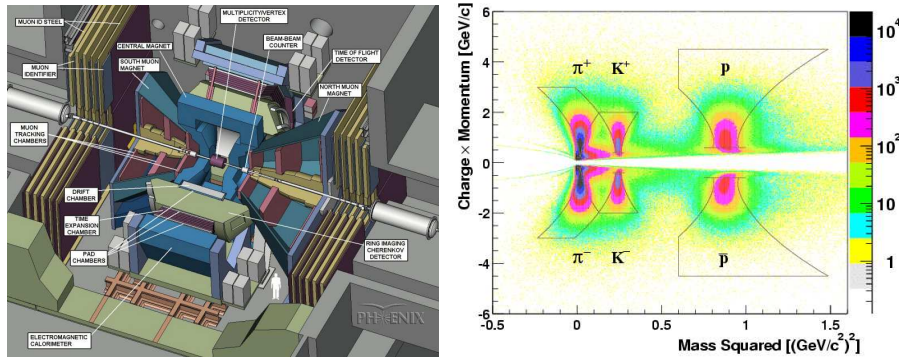
2

Figure 1. a (left): A cutaway drawing of the PHENIX detector. Labeled arrows point to the major detector subsystems. b(right): Mass squared vs. momentum · charge distribution. The lines indicate the PID cut boundaries for pions, kaons, and protons(anti-protons) from left to right, respectively.

tectors (Figure 1a). The east central arm has a unique hadron identification capability in a broad momentum range. Pions and kaons are identified up to 3 GeV/c and 2 GeV/c in p_{T}, respectively, and protons and anti-protons can be identified up to 4.5 GeV/c by using a high resolution time-of-flight detector. In Figure 1b, a plot of m^2 versus momentum multiplied by charge is shown together with applied PID cuts as solid curves.

3. Results

For single particle analysis, we have measured the transverse momentum spectra and yields for $\pi^{\pm}$, $K^{\pm}$, p and $\bar{p}$ at mid-rapidity in Au+Au collisions at $\sqrt{s_{\mathrm{NN}}} = 200$ GeV over a broad momentum range with various centrality selections. Figure 2 shows the p_{T} distributions for pions, kaons, protons, and anti-protons. The top two plots are for the most central 0–5% collisions, and the bottom two are for the most peripheral 60–92% collisions. The spectra for positive particles are presented on the left, and those for negative particles on the right. We have observed a clear particle mass dependence of the shapes of transverse momentum spectra in central collisions below ~ 2 GeV/c in p_{T}. On the other hand, in the peripheral events, the mass dependences of the p_{T} spectra are less pronounced and the p_{T} spectra are more nearly parallel to each other. Another notable observation is that at p_{T} above ~ 2.0 GeV/c in central events, the p and $\bar{p}$ yields become comparable to the pion yields.
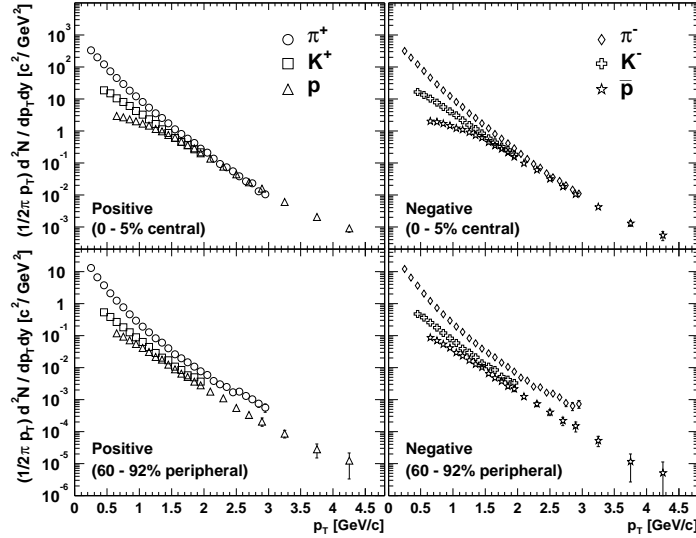
Figure 2. Transverse momentum distributions for pions, kaons, protons and anti-protons in Au+Au collisions at $\sqrt{s_{\mathrm{NN}}} = 200$ GeV.

3.1. *Radial Flow*

In order to deduce radial flow velocity and thermal freeze-out temperature, particle spectra were compared to a functional form, which describes a boosted thermal source, based on relativistic hydrodynamics [3]. This is a two–parameter model, termed the "blast-wave" model, in which the surface radial flow velocity (β_{T}) and freeze-out temperature (T_{fo}) are extracted from the invariant cross section data according to the equation

$$\frac{dN}{m_{\mathrm{T}}\,dm_{\mathrm{T}}} \propto \int_0^R f(r)\,r\,dr\,m_{\mathrm{T}} I_0\Big(\frac{p_{\mathrm{T}}\sinh\rho}{T_{\mathrm{fo}}}\Big) K_1\Big(\frac{m_{\mathrm{T}}\cosh\rho}{T_{\mathrm{fo}}}\Big), \qquad (1)$$

where I_0 and K_1 represent modified Bessel functions with ρ being the transverse boost which depends on the radial position according to $\rho(r) = \tanh^{-1}(\beta_{\mathrm{T}}) \cdot r/R$. To study the parameter correlations, a grid of $(T_{\mathrm{fo}}, \beta_{\mathrm{T}})$ pairs is generated and then a χ^2 minimization is performed for each particle type. The experimental data include the decay of resonance; we add the decay of mesonic ($\rho, \eta, \omega, K^*, , ,$) and baryonic ($\Delta, \Lambda, \Sigma, , ,$) resonance effects, the abundance of which is determined by chemical parameters. The two–dimensional grid search results obtained in this analysis for each centrality bin are shown in Figure 3. The expansion velocity parameter is seen
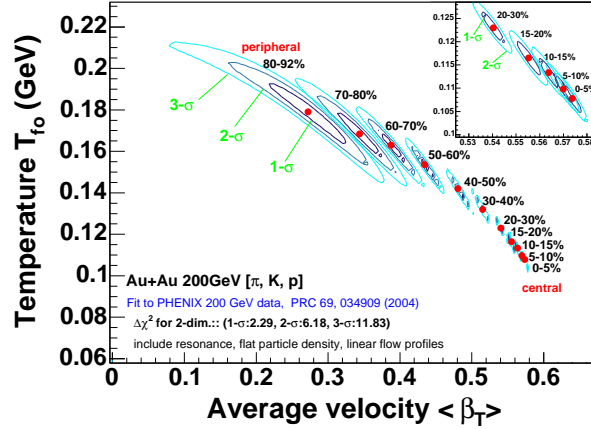
4

Figure 3.   Contour plots for hydrodynamical fit to 200 GeV single particle transverse momentum spectra. The contour lines are in standard deviation steps.

to decrease moderately toward peripheral collisions and the kinetic freeze-out temperature increases significantly, approximately 40%. If one takes these parameters literally, then radial flow is weak in the peripheral collisions and the particles decouple kinetically from each other at temperatures close to the chemical freeze-out temperature. This is a physically reasonable scenario given the small number of participants in the initial expansion phase. For the most central 0–5% collisions, we have obtained freeze-out temperature $T_{\rm fo} = 108$ MeV and average flow velocity $\langle \beta_{\rm T} \rangle = 0.57$.

3.2. High-$p_{\rm T}$ Hadron Production

For the high-pt region, the scaling behavior of identified charged hadrons has been compared with results for neutral pions. Figure 4 shows the central (0–10%) to peripheral (60–92%) ratio for $N_{\rm coll}$ (number of collisions) scaled $p_{\rm T}$ spectra of $(\bar{p} + p)/2$, kaons, charged pions, and π^0. We define R_{CP} as:

$$R_{CP} = \frac{\text{Yield}^{0-10\%}/\langle N_{\rm coll}^{0-10\%} \rangle}{\text{Yield}^{60-92\%}/\langle N_{\rm coll}^{60-92\%} \rangle}. \qquad (2)$$

The data show that $(\bar{p} + p)/2$ reaches unity for $p_{\rm T} > 1.5$ GeV/c, consistent with $N_{\rm coll}$ scaling. The data for kaons also show the $N_{\rm coll}$ scaling behavior around $1.5 - 2.0$ GeV/c, but the behavior is weaker than for protons. However, the neutral and charged pions are suppressed at $2 - 3$ GeV/c with respect to peripheral Au+Au collisions.
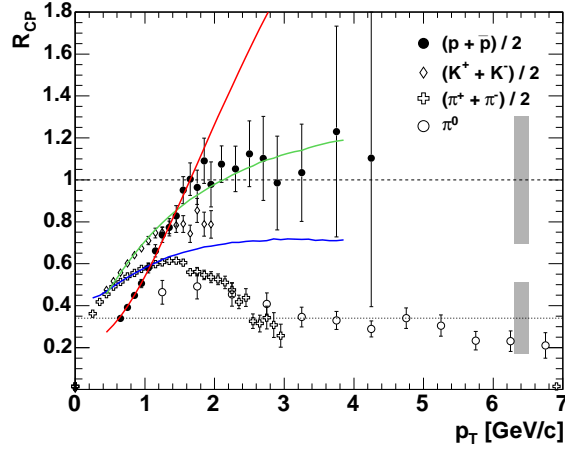
Figure 4. R_{CP} as a function of p_T for $(\bar{p} + p)/2$, charged kaons, charged pions, and π^0. The horizontal lines indicate the expectations of N_{part} (dotted) and N_{coll} (dashed) scaling, the shaded bars represent the systematic errors on these quantities. The curves on data are calculated by blast–wave fit results.

The standard picture of hadron production at high momentum is the fragmentation of energetic partons. While the observed suppression of the π yield at high p_T in central collisions may be attributed to the energy loss of partons during their propagation through the hot and dense matter created in the collisions, i.e. jet quenching, it is a theoretical challenge to explain the absence of suppression for baryons up to 4.5 GeV/c for all centralities along with the enhancement of the p/π ratio at $p_T = 2$ – 4 GeV/c for central collisions. The observed R_{CP} in intermediate p_T region are not explained by the hydrodynamic model alone, but some of theoretical model qualitatively agree with data. These observations can be explained by the hydrodynamical model with jet fragmentation (hydro + jet model) [4] and the parton recombination at intermediate p_T (recombination model) [5]. Both theoretical models reproduce the binary collision scaling observed in the data.

References

1. PHENIX Collaboration, S.S. Adler *et al.*, Phys. Rev. **C 69** 034909 (2004).
2. K. Adcox *et al.*, Nucl. Instrum. Methods A **499** 469 (2003).
3. E. Schnedermann, J. Sollfrank, and U. Heinz, Phys. Rev. **C 48** 2462 (1993).
4. T. Hirano and Y. Nara, Phys. Rev. **C 69** 034908 (2004).
5. R. J. Fries, B. Müller, C. Nonaka, S. A. Bass, Phys. Rev. **C 68** 044902 (2003).